MICROFIBRIL AGGREGATES IN PRETREATED BAMBOO FIBERS ANALYZED WITH ATOMIC FORCE MICROSCOPY

Hong Chen†
Lecturer
Furniture and Industrial Design College
Nanjing Forestry University
Nanjing, China
E-mail: chenhong@njfu.edu.cn

Genlin Tian
Research Associate
International Centre for Bamboo and Rattan
Chaoyang District
Beijing, China
E-mail: tiangenlin@icbr.ac.cn

*Zhihui Wu**
Professor
Furniture and Industrial Design College
Nanjing Forestry University
Nanjing, China
E-mail: wzh550@sina.com

*Benhua Fei**†
Professor
International Centre for Bamboo and Rattan
Chaoyang District, Beijing, China
E-mail: feibenhua@icbr.ac.cn

(Received August 2015)

Abstract. Fibers of primary cell walls of Ci bamboo (*Neosinocalamus affinis*) were analyzed with an atomic force microscope (AFM) to determine the arrangement of microfibril aggregates and the effect of pretreatments (ultrasonic treatment and different drying methods) on the arrangement and diameter of microfibril aggregates and the cell wall topography. The microfibril aggregates in primary cell walls of bamboo fiber showed a randomly interwoven structure. Differences in the spacing between microfibril aggregates observed from the AFM phase images and the diameters of microfibril aggregates determined from the AFM height topography of the nanostructure of primary cell walls of bamboo fiber were found relevant to the pretreatments during the sample preparation. The microfibril aggregates in primary cell walls of bamboo were actually the aggregations of different numbers of cellulose fibrils. Also, the ultrasonic treatment could have increased the roughness of bamboo fiber and exposure of microfibril aggregates. The data suggest that sample preparation and pretreatments should be considered relevant to the arrangement and diameter of microfibril aggregates as well as the topography in studying the nanostructure of cell walls with AFM.

Keywords: Bamboo fiber, microfibril aggregate, atomic force microscope.

* Corresponding author
† SWST member

© 2016 by the Society of Wood Science and Technology

INTRODUCTION

Bamboo fiber is a natural, biological material with the unique polylamellate structure of alternating broad and narrow lamellae as well as superior mechanical properties, which is important in designing composite materials (Parameswaran and Liese 1976; Zhou 1996; Wang et al 2011). Bamboo fiber is a promising alternative for reinforcing fibers in composites and for the pulp and paper industry because of its low density, good mechanical performance, fast growth rate, and environmental friendliness (Mohanty et al 2000; Aranberri-Askargorta et al 2003; Chen et al 2011). Therefore, studying microfibril aggregates, which are the elementary components in primary cells of bamboo fiber, is very important.

Atomic force microscope (AFM) is a promising tool for studying biological materials. AFM is capable of obtaining images with nanometer resolution under native or near native conditions and is therefore ideal for studying cell walls (Kirby et al 1996; Cybulska et al 2010; Zhang et al 2012). Native microfibrils were studied in both air-dried and freeze-dried samples by AFM in a number of studies. Yu et al (2008a, b) revealed that cellulose microfibrils in parenchyma cell walls of wheat straw have an interwoven network texture, which was obtained by AFM phase image. Cybulska et al (2013) studied the relationship between the nanostructure of cell walls and their texture for six different apple cultivars. They measured the diameter of cellulose microfibrils based on the AFM height topographs obtained using tapping mode. Fahlén and Salmén (2003, 2005) studied the arrangement of cellulose aggregates in the secondary cell wall layer of spruce wood as well as the effects of chemical and mechanical processing on the pore, matrix structure, and arrangement of cellulose microfibrils by observing the cross section of fibers with AFM. Then, also observing the cross section of spruce wood fiber with AFM, Zimmermann et al (2006) discovered that the arrangement of cellulose microfibrils strongly depended on the pretreatment and preparation of samples. The examination of microfibrils with AFM allowed accurate determination of fibril widths as 1.0-2.0 nm reported by Niimura et al (2010).

Kirby et al (1996), Davies and Harris (2003), and Kontturi and Vuorinen (2009) used AFM to study the structure of partially dried and isolated cell wall fragments. Pesacreta et al (1997) investigated the effect of chemical treatment on cell wall organization and topography in either air or water with AFM. Water and pectin content in cells significantly influenced the diameter of cellulose microfibrils, which was documented in an experiment with different water levels of hydration and selective removal of pectins (Thimm et al 2000, 2009). AFM was also applied for studying the action of cellulose enzyme on cellulose, which showed an increase in the proportion of crystalline regions during hydrolysis (Liu et al 2009). Despite a number of studies on different kinds of cell walls with AFM, there are only three studies of cell walls of bamboo fiber with AFM because of its complicated structure and the difficulty in preparing samples. Two studies (Yu et al 2008a; Chen et al 2014) investigated the arrangement of cellulose microfibrils in Moso bamboo (*Phyllostachys pubescens*). They found that cellulose microfibrils were randomly oriented in the primary cell wall. For bamboo fibers, AFM was also a powerful tool for the high-resolution observation of the microfibrils. Another study reported the discovery of cobble-like polygonal cellulose nanograins with diameters of 21-198 nm in the cell walls of bamboo fibers (*Phyllostachys edulis*) (Zou et al 2009).

Studying cellulose microfibril aggregates in primary cell walls of bamboo fiber using AFM will be increasingly important in the future. But, the first problem to be tackled is how to prepare samples and finding out if the common pretreatments affect the microfibril aggregates in cell walls of bamboo fiber. *Neosinocalamus affinis* is a common bamboo that is usually used for making paper, textiles, fiber-reinforced composites, etc. Therefore, in this study, bamboo (*N. affinis*) fibers were investigated to determine the arrangement of microfibril aggregates in primary cell walls and the effect of the four pretreatments on microfibril aggregates.

EXPERIMENTAL PROCEDURES

Materials and Methods

Materials were obtained from the area between the lines shown in Fig 1 in 1-yr-old bamboo culms grown in a plantation with 3500 bamboos per hectare in Taiping, Huangshan City, Anhui Province, China. There were two reasons for choosing 1-yr-old culms: 1) full lignification of the component cell completes within one growing season (Itoh 1990) and 2) hardness of bamboo fiber in 1-yr-old bamboo is less than that of 2- or 3-yr-old ones, which is beneficial for preparing samples. Bamboo taken 2 m from the bottom of the culms was cut into strips (30 mm longitudinally and 2 × 2 mm in cross section). Then the strips were immersed into solution and kept at 65°C for 18.5 h to isolate the bamboo fibers (Wang et al 2011). The solution was prepared with one part 30% hydrogen peroxide (H_2O_2) and one part 100% glacial acetic acid (HAc), which can remove lignin more effectively than other chemical methods (Chen et al 2013). Bamboo fibers were washed with deionized water to neutrality. In our previous study, the length of fiber isolated from the area between the lines shown in Fig 1 was from 2 to 3 mm, and the average area of bamboo cell wall was 72.54 nm^2 (Chen 2011).

Pretreatments

The isolated bamboo fibers were dispersed in deionized water and divided in two parts. The fibers in one part were then treated by ultrasound, and the other part was not treated. The ultrasonic treatment was made with a high-frequency ultrasonic cell disrupter (JY99-IIND; Ningbo Scientz Biotechnology Co. Ltd., Zhejiang Province, China) operated at 19.5-20.5 kHz with an output of 600 W, and the treatment was kept up for 5 s with 5-s stopping intervals for 30 min. Both untreated and treated fiber suspensions were dropped on a clean glass slide for air-drying for 24 h. Other fiber suspensions, also both untreated and treated, were frozen in liquid nitrogen followed by drying for 40 h in a freeze dryer.

Sample Preparation for Tapping Mode AFM

The freeze-dried fibers were put on the glass slide with double-sided tape using fine-tipped tweezers under a microscope. The air-dried fibers were stuck to the glass slice because of van der Waals force during the drying process, which could be observed with AFM directly.

An Icon AFM (Burker Corporation, Santa Barbara, CA) was used to study the microfibrils on primary cell walls of bamboo fiber. The specimens were scanned under tapping mode using sharp tapping mode probes with a tip radius of 8 nm. The length of the cantilever was 125 um, the spring constant was 42 N/m, and the resonant frequency was 320 kHz. The samples were scanned at room temperature of 23°C ± 2°C and ambient humidity of 35% ± 5%. Images were

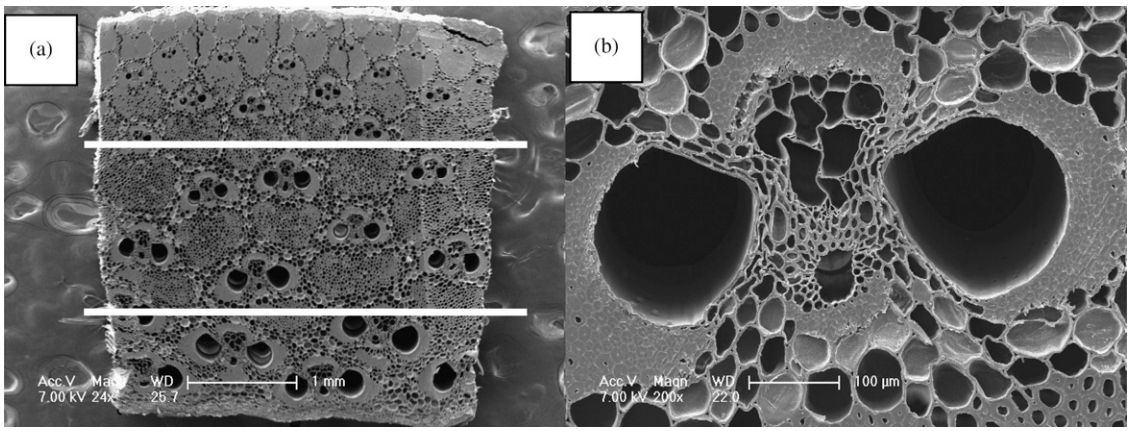

Figure 1. Cross-section of (a) bamboo culm and (b) the vascular bundle.

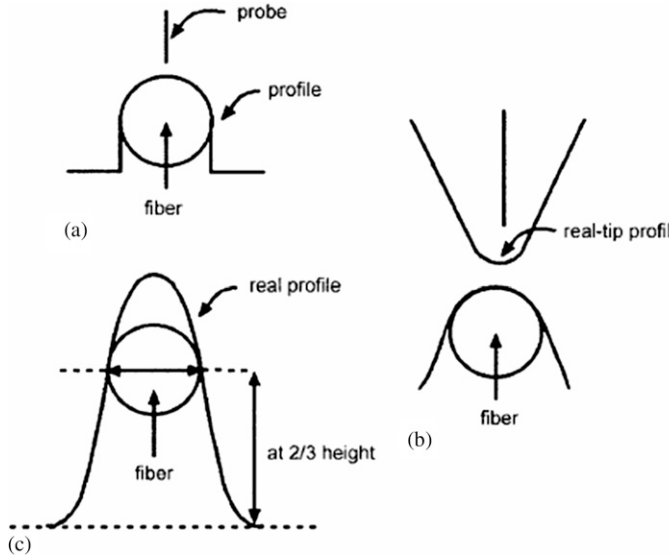

Figure 2. Effect of tip size on the measurement of microfibril diameter. (a) Measuring with an infinitely sharp tip, (b) measuring with a tip of diameter similar to that of the fiber, and (c) diameter measured at 2/3 of image height (Thimm et al 2000).

captured as 512 × 512 pixel images for a 1.0-μm- or 500-nm-wide square. Real-time scanning was performed with scan rates of 1.0 Hz, scan angle of 0°, and tapping frequencies ranging from 340 to 380 KHz. Images were obtained in both the height mode, in which the deflection of the cantilever was directly used to measure the *z* position, and in the phase mode, in which the phase lag was used to determine differences in materials, as presented by Fahlén and Salmén (2005).

Measurement of Roughness and Microfibril Aggregate Diameter

The images were acquired and processed by the instrument software. Images were flatted by the software in AFM for better visibility, which did not affect precision of contour measurement.

Using the software, roughness of fibers was measured from 10 independent images scanned from each sample of Ci bamboo fiber. The microfibril aggregate diameters were measured. For the problems associated with this type of measurement, the methods described by Thimm et al (2000) were applied in this study, which solved the probe enlargement effect to a certain degree (Fig 2), and eventually, diameters of the microfibril aggregates at 2/3 height were obtained. Diameters of 40 microfibrils were measured in five fibers randomly selected.

RESULTS AND DISCUSSION

Morphology of Bamboo Cell Walls Influenced by Different Pretreatments

Figure 3 shows that all cell walls had shrinkage in the surface, but the shrinkage was different for different pretreatments. The shrinkage possibly resulted from the loss of the chemical component, which made more spaces and pores among the microfibril aggregates. When dried, the microfibrils aggregated together, which was observed as shrinkage macroscopically. In our previous study (Chen et al 2011, 2013), there was almost no shrinkage in bamboo cell walls isolated mechanically, which proved that the most probable reason for shrinkage was the loss of almost all lignin and part of the hemicellulose. The surfaces treated and untreated by ultrasonic were different regardless of the drying method. The shrinkage of the cell wall treated by ultrasonic was more than that of the untreated, which was

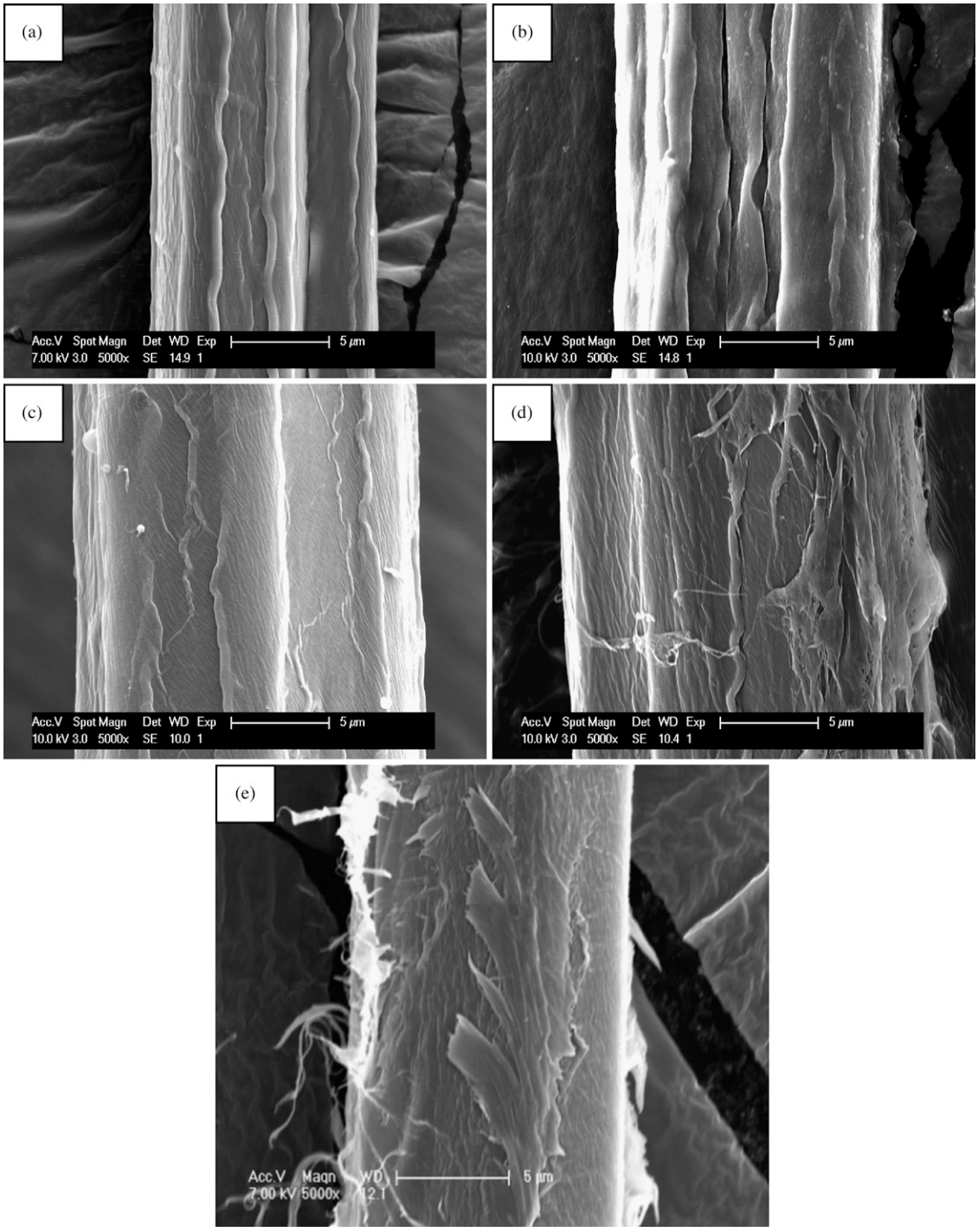

Figure 3. Typical field emission scanning electron microscope images of bamboo fiber treated differently. (a) Untreated and air-dried, (b) treated and air-dried, (c) untreated and freeze-dried, (d) treated and freeze-dried, and (e) isolated mechanically (Chen et al 2011).

in agreement with the results obtained by our previous study (Chen et al 2011). The dry method also affected the morphology of the cell wall. There was much smaller shrinkage in freeze-dried bamboo cell walls compared with air-dried. All the changes caused by shrinkage actually resulted from the change of microfibril aggregates, which is discussed in detail in the following section.

Arrangement of Cellulose Microfibril Aggregates in Bamboo Fiber Primary Cell Walls

In the height images (Fig 4a and c), microfibril aggregates are clearly visible. The yellow scale represents differences in microfibril height, in which lighter areas mean higher and darker regions lower. This is a good indicator of how flat a sample was (Thimm et al 2009). In the phase

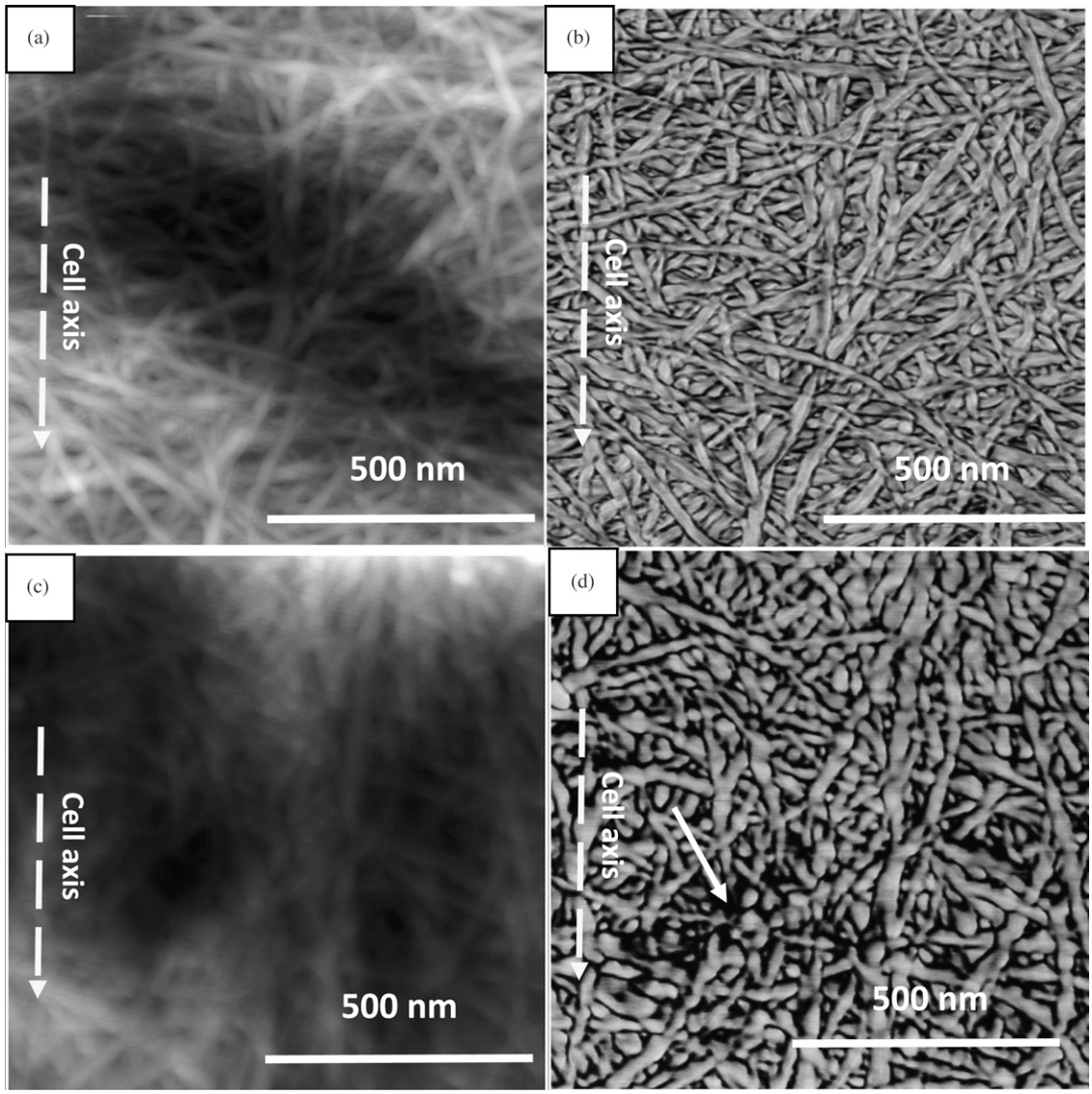

Figure 4. AFM (a and c) height images and (b and d) phase images of cellulose microfibril in primary cell walls of bamboo fiber; (a) and (b) are Ci bamboo fiber, (c) and (d) are Moso bamboo fiber.

images (Fig 4b and d), individual microfibril aggregates were observed as bright areas corresponding to regions of greater stiffness. Both the hemicellulose–lignin matrix and the gaps between microfibril aggregates are shown as dark areas surrounding the bright and stiffer microfibril aggregates shown by arrows in Fig 4d. Both these components were known to have lower stiffness than cellulose (Fahlén and Salmén 2003, 2005).

Figure 4a and b shows height and phase images of microfibril aggregates, respectively, on the primary cell walls of Ci bamboo, a typical species of monopodial bamboo. For comparison, the height image and the phase image of microfibril aggregates of Moso bamboo, which is a typical species of sympodial bamboo, are also presented in Fig 4c and d. In all of the images, microfibril aggregates are visible as the brighter and more elongated objects. Whether in the height images or phase images, it was shown that microfibril aggregates on the primary cell walls of both Ci and Moso bamboos overlap, forming an interwoven structure, which was consistent with the findings of Yu et al (2008a) who studied air-dried Moso bamboo fiber.

AFM images in Fig 4, especially the phase images, which often showed surface features invisible or barely visible in height images (Hansma et al 1997), clearly showed the microfibril aggregates in the primary cell walls of bamboo fiber. All images indicated that the microfibril aggregates in the primary cell walls of bamboo fiber had an interwoven network texture, in which the microfibril aggregates interwove tightly and randomly. The interwoven network texture was similar to the structure of primary cell walls of onion and *Arabidopsis thaliana* (L.) (Davies and Harris 2003), wheat straw (Yu et al 2008b), and some apple species (Cybulska et al 2013) but less aligned than that in primary cell walls of Chinese water chestnut, potato, and carrot (Baker et al 1998) and parenchyma cell walls of celery (*Apium graveolens* L.) (Thimm et al 2000, 2009). In addition, the arrangement of primary cell walls of bamboo fiber was similar to that of wood fiber, which has been studied more and built as a widely accepted model (Kerr and Goring 1975). Such an arrangement of cellulose microfibril aggregates was helpful to keep the cell wall in shape and strengthen the cell wall (Yu et al 2008b).

Microfibril aggregates in the secondary cell wall are shown in Fig 5. The arrangement of microfibril aggregates aligned in order, which was different from that in the primary cell wall. Currently, it is

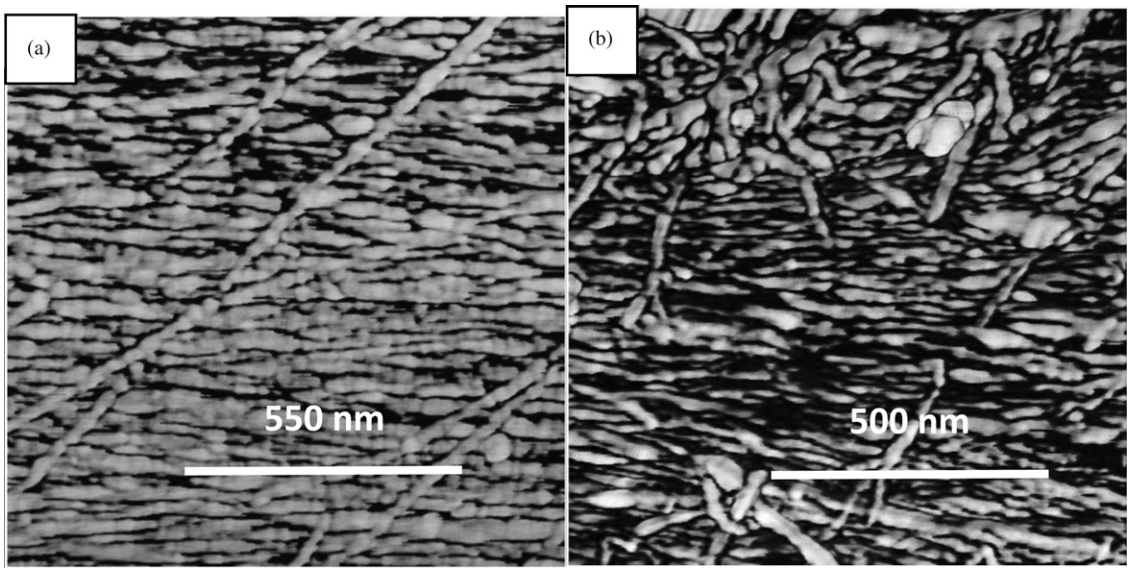

Figure 5. Arrangement of microfibril aggregates of two random layers (a and b) in secondary walls of bamboo fiber.

difficult to obtain the arrangement of microfibril aggregates in secondary cell wall due to the limitation of the technique. The condition of microfibril aggregation of each layer in the secondary bamboo cell wall needs further study.

Microfibril Aggregates in Primary Cell Walls of Bamboo Fiber with Different Pretreatments

Spacing between microfibril aggregates. AFM phase images of bamboo fibers with different pretreatments are shown in Fig 6. In spite of all images clearly showing a similar randomly interwoven structure, the microfibril aggregates presented differently, especially concerning the spacing among microfibril aggregates. Compared with that in freeze-dried samples, the microfibril aggregates in air-dried samples pressed each other much closer, especially in the samples treated by ultrasound. In addition, for air-dried samples (Fig 6a and b), the microfibril aggregates

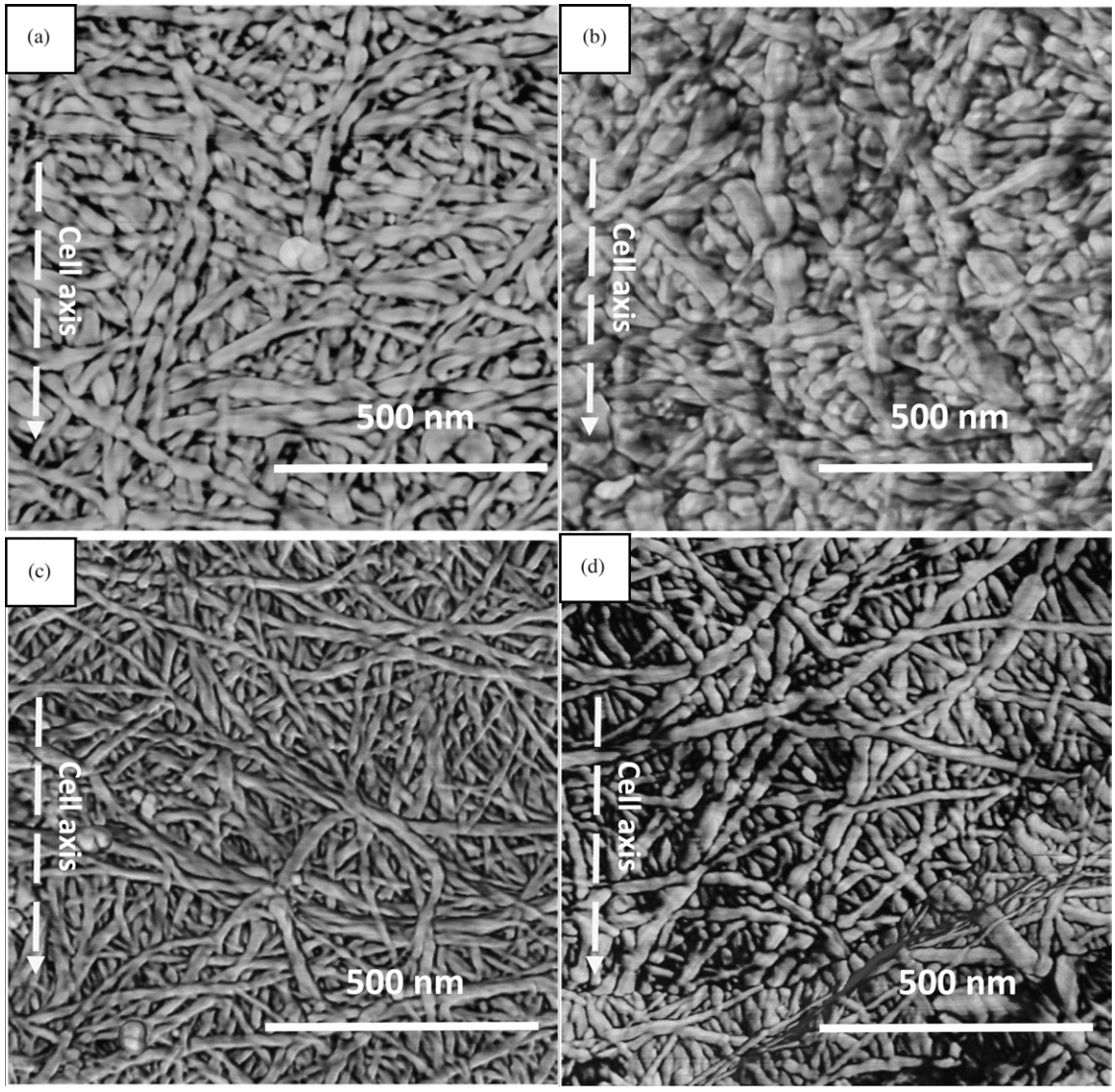

Figure 6. AFM phase images at 500 nm of cellulose microfibrils with different pretreatments. (a) Untreated and air-dried, (b) treated and air-dried, (c) untreated and freeze-dried, and (d) treated and freeze-dried.

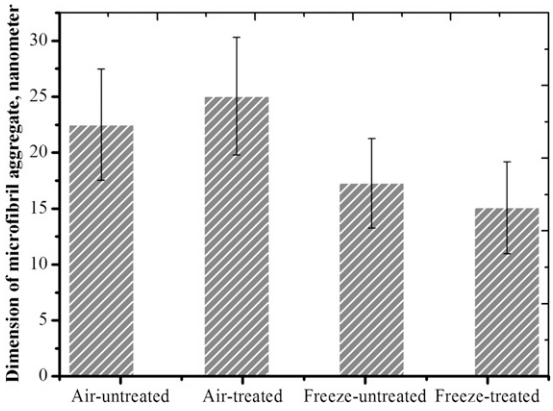

Figure 7. Diameters of cellulose microfibril aggregates in primary cell walls of bamboo fiber.

in fibers treated by ultrasound pressed each other tighter than that in untreated samples, which meant smaller spacing among microfibril aggregates treated. However, the phenomenon shown in freeze-dried samples (Fig 6c and d) was in contrast with the air-dried samples. Namely, the spaces between microfibril aggregates in treated samples were larger than those in untreated ones.

The bamboo fiber cell wall was isolated by H_2O_2 and HAc, which removed partially noncellulosic polysaccharides and did not cause the swelling of microfibrils (Emons 1988). Removal of cell wall components decreased the ability of the fragment to retain water, accelerating water loss. Air-drying the bamboo fiber overnight under ambient conditions resulted in high levels of water loss and aggregation (Kirby et al 2006). However, there was no gross change on structure induced by freeze-dried during sample preparations (Kirby et al 1996). Therefore, there were many differences of spacing among microfibril aggregates between air-dried and freeze-dried samples (Fig 6).

Ultrasound can have acoustic cavitation effect, mechanical vibration, thermal effect, etc (Weissler 1984). The acoustic cavitation effect of high-frequency ultrasound can produce thousands of pascals of pressure, which could cause the compression of microbubbles which then explode in a second (Weissler 1984; Mo et al 2009). The whole process accelerated extracting the targeted extractive. Meanwhile, the mechanical vibration and thermal effect promoted the dissolution ingredient to diffuse (Gong 1999; Liu et al 2003). As a consequence, the ultrasonic treatment achieved an intensive mechanical fibrillation, isolated more noncellulosic polysaccharides from the microfibrils, and induced more gaps among the cellulose microfibril aggregates. In air-dried samples after ultrasonic treatment, the microfibril aggregates overlapped tightly for loss of water and shrinkage (Fig 6b). However, the microfibril aggregates in treated and freeze-dried samples were arranged loosely for losing more noncellulosic polysaccharides, which resulted in larger gaps among cellulose microfibril aggregates (Fig 6d).

Diameter of microfibril aggregates. Microfibril diameters were measured from the plot profiles of AFM height images as shown in Fig 7. The results analyzed statistically are shown in Table 1. Figure 7 shows that the thickness of cellulose microfibril aggregates in air-dried samples registered more than 20 nm, whereas that in freeze-dried samples stood at less than 20 nm. Diameters of cellulose microfibril aggregates in air-dried untreated samples were smaller than those in treated ones. Although for the same freeze-dried samples, microfibril aggregate diameters in untreated samples were greater than those in treated ones. Such a phenomenon was also observed in AFM phase images (Fig 8). Furthermore, Table 1 indicates that the diameter of treated microfibril aggregates were significantly different as well.

A number of studies with AFM suggested that the mean diameter of the microfibrils were in

Table 1. Diameters of microfibril aggregates with different treatments were analyzed statistically.

	SS	df	MS	F	p-value	F_{crit}
Between groups	3508.75	3	1169.58	87.35	3.87	2.68
Within groups	1620.19	121	13.39	—	—	—
Total	5128.94	124				

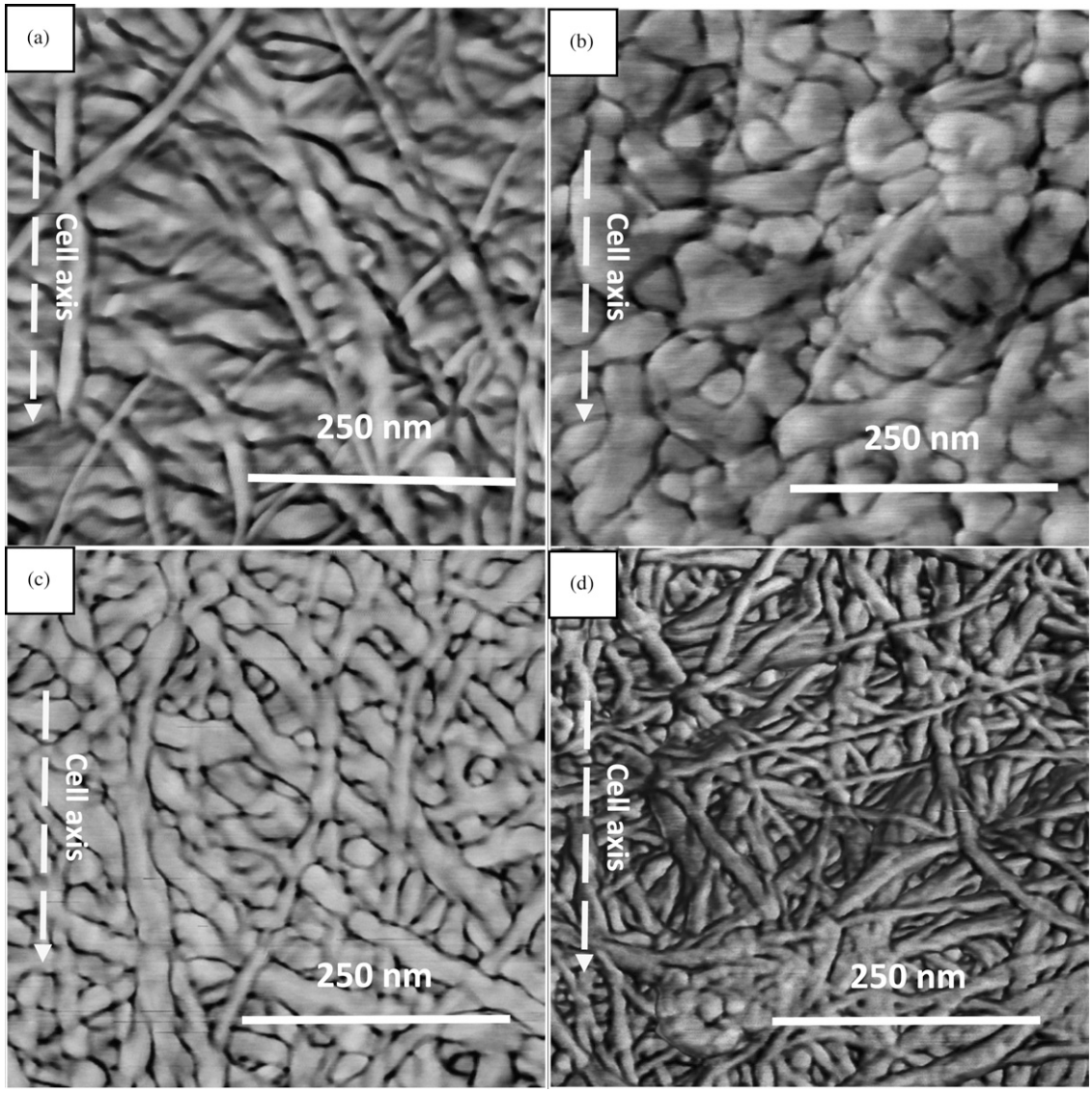

Figure 8. AFM phase images at 250 nm of cellulose microfibrils with different pretreatments. (a) Untreated and air-dried, (b) treated and air-dried, (c) untreated and freeze-dried, and (d) treated and freeze-dried.

the range of 20-40 nm in air-dried primary cell walls of different plants (cotton, celery, apple, and wheat straw) (Pesacreta et al 1997; Thimm et al 2000; Yu et al 2008b; Cybulska et al 2013). Diameters of microfibril aggregates in air-dried bamboo fiber in this study were consistent with former measurements in other plant cell walls. In addition, the diameter of microfibril aggregates in freeze-dried cell walls of plants was examined in many previous studies (Thimm et al 2000; Fahlén and Salmén 2003, 2005). Fahlén and Salmén investigated the mean diameter of microfibrils in spruce wood, which reached about 18 and 16 nm in cross sections of different samples in 2003 and 2005, respectively. Average diameters of microfibril aggregates in freeze-dried samples were about 17 and 15 nm in untreated and treated samples, respectively, obtained in

this study, which was similar to Fahlén and Salmén's results.

As with many kinds of plant cell walls, especially wood cell walls, microfibrils in the cell walls of bamboo fiber were embedded in a complex matrix of noncellulosic polysaccharides, which mainly included hemicellulose and lignin (Liese 2015). As a part of the fiber structure, water probably served to stabilize fiber and polysaccharide structures through hydrogen bonding. In the structure of bamboo cell walls, hydrogen bonding probably played the most important part. In air-drying, loss of water caused the loss of native structure, triggering increased coating and aggregation. Therefore, the explanation of the larger diameter in air-dried samples was that during dehydration, microfibrils aggregated together and/or noncellulosic polysaccharides accumulated on the surfaces of microfibril aggregates, leading to more coating (Thimm et al 2000).

However, Thimm et al (2000) indicated that the average microfibril diameter of about 35 nm in freeze-dried celery was greater than that of 23 nm in air-dried celery. It was in contrast to our results that the diameter of microfibril aggregates in freeze-dried samples was smaller than that of air-dried ones. Different sample preparation procedure could have been the reason; samples were cut into cross section in Thimm's research, whereas ours were isolated by H_2O_2 and HAc without any cutting. But our results of freeze-dried samples were consistent with the average microfibril aggregate diameter of about 15 nm in hydrated walls of celery in the same study by Thimm et al (2000).

As reported by Kirby et al (1996), there was no gross change of structure induced by freeze-drying during sample preparations. In contrast to treated samples with the same freeze-drying, diameters of microfibril aggregates in untreated samples were larger because of the likelihood that noncellulosic polysaccharides associated with the surface of the cellulose in untreated cell walls (Davies and Harris 2003), because ultrasonic treatment probably isolated more noncellulosic polysaccharides from not only the cell wall but also from the surfaces of microfibril aggregates.

In this study, all average diameters of cellulose microfibril aggregates, regardless of the pretreatment, were more than 15 nm. However, many researchers reported that the cross-sectional diameters of cellulose I crystallites were in the range of 2-3 nm (Newman et al 1994, 1996; Koh et al 1997). Hemicelluloses such as xyloglycans, xylans, etc. were known to adhere to microfibrils and interlink them with nonbranched regions via hydrogen bonds. The partial removal of lignin and hemicellulose would enable the microfibrils to move closer together within the cell wall; thus microfibrils had a greater tendency to self-associate, which probably resulted in greater aggregation (Thimm et al 2009). Kirby et al (2006) determined that after sequential extraction of the pectin, partial extraction of xyloglucan, and almost complete removal of xyloglucan of potato, the interfiber spacing decreased from 20.2 to 11 nm. Davies and Harris (2003) determined that the diameter of microfibrils decreased to 3.2 nm when the pectic polysaccharides were removed in *A. thaliana* cell walls. All the findings indicate that aggregation and the coating and/or the linkage existed between cellulose microfibrils and noncellulosic polysaccharides in bamboo fiber primary walls. Therefore, this study supported such findings, ie, the microfibril aggregates observed in AFM were actually assemblies of different numbers of cellulose elementary fibrils, which was consistent with that obtained from the cross section of wood fibers by Fahlén and Salmén (2003, 2005).

Roughness of bamboo fiber primary cell wall. Table 2 indicates that the roughness of primary cell walls of bamboo fiber was different after different pretreatments. Both Ra, arithmetic average of the absolute values of the surface height deviations measured from the mean plane, and Rmax, maximum vertical distance from the highest to the lowest data points in the image following the planefit, of the treated fibers were greater than those of untreated ones regardless of how the samples were dried. For untreated samples, Ra and Rmax of air-dried

Table 2. Roughness of bamboo fiber primary cell wall.[a]

	Air-dried				Freeze-dried			
	Untreated		Treated		Untreated		Treated	
Index	Ra (nm)	Rmax (nm)	Ra (nm)	Rmax (nm)	Ra (nm)	Rmax (nm)	Ra (nm)	Rmax (nm)
	8.62 (0.73)	97.15 (0.73)	14.37 (0.54)	111.45 (0.71)	5.52 (0.36)	52.02 (0.15)	29.80 (0.88)	175.74 (0.49)

[a] Numbers in parentheses are coefficients of variation.

fibers were a little greater than those of freeze-dried ones; however, the trend was in contrast with that in treated samples, namely, both Ra and Rmax of air-dried fibers were lower compared with those of freeze-dried samples.

For untreated samples, compared with freeze-dried fiber, there were more aggregations among microfibrils and associations of noncellulosic polysaccharides with the surface of microfibrils in air-dried samples, which resulted in greater roughness in air-dried samples. However, both treated samples presented more spacing among microfibrils in freeze-dried samples; therefore, the roughness was greater than untreated. Ultrasonic treatment increased the roughness of bamboo fiber and wettability, which was consistent with the results of our previous study that the ultrasonic treatment decreased the water contact angle of single bamboo fibers (Chen et al 2011). The greater roughness contributed to a lower contact angle and thus a greater surface free energy, which greatly contributed to an increase of adhesion by improving wettability (Silva and Al-Qureshi 1999).

CONCLUSIONS

The microfibril aggregates in primary cell walls of bamboo fiber overlap, forming a randomly interwoven structure observed with AFM. Both the ultrasonic treatment and the drying methods, namely the pretreatments, affect the arrangement and diameter of microfibril aggregates observed by AFM. The microfibril aggregates in bamboo primary cell walls observed by AFM are the aggregations of different numbers of cellulose fibrils. Furthermore, ultrasonic treatment can increase roughness of bamboo fiber and exposure of microfibril aggregates, which provides insight on enhancing wettability of bamboo fiber and observing microfibril aggregates. Therefore, it is possible to observe the nanoscale characteristics in bamboo fiber cell walls, especially the microfibril aggregates, using AFM, and it is important to choose the appropriate procedure of sample preparation.

ACKNOWLEDGMENTS

This work was funded by the National Natural Science Foundation of China (31500474), National Natural Science Foundation of China (31370563), Jiangsu Natural Science Foundation of China (No. BK20150881), and the Priority Academic Program Development of Jiangsu Higher Education Institutions (PAPD). The authors appreciate Gao Nuoli from International Centre for Bamboo and Rattan for helping to revise the manuscript carefully to avoid grammar or syntax error.

REFERENCES

Aranberri-Askargorta I, Lampke T, Bismarck A (2003) Wetting behavior of flax fibers as reinforcement for polypropylene. J Colloid Interface Sci 263(2):580-589.

Baker AA, Helbert W, Sugiyama J, Miles MJ (1998) Surface structure of native cellulose microcrystals by AFM. Appl Phys A-Mater 66:S559-S563.

Chen H (2011) The relationship between properties of single bamboo fibers and preparation methods. MS thesis, Chinese Academy of Forestry, Beijing, China. 18 pp.

Chen H, Fei BH, Cheng HT, Jiang ZH, Wang G (2013) The implication of different chemical treatments on chemical components of bamboo fibers. China Forest Prod Ind 40(3):49-52.

Chen H, Tian GL, Fei BH (2014) The arrangement of cellulose microfibrils in primary cell wall of Moso bamboo fiber studied with AFM. Scientia Silvae Sinicae 50(3):90-94.

Chen H, Wang G, Cheng HT (2011) Properties of single bamboo fibers isolated by different chemical methods. Wood Fiber Sci 43(2):1-10.

Cybulska J, Konstankiewicz K, Zdunek A, Skrzypiec K (2010) Nanostructure of natural apple cell wall and model cell wall materials. Int Agrophys 24:107-114.

Cybulska J, Zdunek A, Psonka-Antonczyk KM, Stokke BT (2013) The relation of apple texture with cell wall nanostructure studied using an atomic force microscope. Carbohydr Polym 92:128-137.

Davies LM, Harris PJ (2003) Atomic force microscopy of microfibrils in primary cell walls. Planta 217:283-289.

Emons ACM (1988) Methods for visualizing cell-wall texture. Acta Bot Neerl 37:31-38.

Fahlén J, Salmén L (2003) Cross-section structure of the secondary wall of wood fibers as affected by processing. J Mater Sci 38:119-126.

Fahlén J, Salmén L (2005) Pore and matrix distribution in the fiber wall revealed by atomic force microscopy and image analysis. Biomacromolecules 6:433-438.

Gong C (1999) Ultrasound induced cavitation and sonochemical effects. PhD dissertation, Massachusetts Institute of Technology, Cambridge, MA. 137 pp.

Hansma HG, Kim KJ, Laney DE, Garcia RA, Argaman M, Allen MJ, Parsons SM (1997) Properties of biomolecules measured from atomic force microscope images: A review. J Struct Biol 119:99-108.

Itoh T (1990) Lignification of bamboo (*Phyllostachys heterocycla* Mitf.) during its growth. Holzforschung 44:191-200.

Kerr AJ, Goring DAI (1975) The ultrastructural arrangement of the wood cell wall. Cell Chem Technol 9:563-573.

Kirby AR, Gunning AP, Waldron KW, Morris VJ, Ng A (1996) Visualization of plant cell walls by atomic force microscopy. Biophys J 70:1138-1143.

Kirby AR, Ng A, Waldron KW, Morris VJ (2006) AFM investigation of cellulose fibers in Bintje potato (*Solanum tuberosum* L.) cell wall fragments. Food Bioph 1:163-167.

Koh TH, Melton LD, Newman RH (1997) Solid-state 13C NMR characterization of cell walls of ripening strawberries. Can J Bot 75:1957-1964.

Kontturi E, Vuorinen T (2009) Indirect evidence of supramolecular changes within cellulose microfibrils of chemical pulp fibers upon drying. Cellulose 16:65-74.

Liese W, Kohl M, eds. (2015) Bamboo. The plant and its uses. Springer International Publishing, Cham, Switzerland.

Liu H, Fu S, Zhu JY, Li H, Zhan H (2009) Visualization of enzymatic hydrolysis of cellulose using AFM phase imaging. Enzyme Microb Technol 45:274-281.

Liu L, Zhang X, Huang Y, Jiang B, Zhang Z (2003) Effect of ultrasonic treatment on surface characteristics of aramid. Acta Mater 20(2):35-40.

Mo X, Huang L, Tian F, Ma L, Ou L, Huang S (2009) Ultrasonic extraction of the total alkaloid from the *Zanthoxylum nitidum*. Chin Wild Plant Resour 28(5):58-62.

Mohanty K, Misra M, Hinrichsen G (2000) Biofibres, biodegradable polymers and biocomposites: An overview. Macromol Mater Eng 276/277:1-24.

Newman RH, Davies LM, Harris PJ (1996) Solid-state 13C nuclear magnetic resonance characterization of cellulose in the cell walls of *Arbidopsis thaliana* leaves. Plant Physiol 111:475-485.

Newman RH, Ha MA, Melton LD (1994) Solid-state 13C NMR investigation of molecular ordering of cellulose in the cellulose of apple cell walls. J Agric Food Chem 42:1402-1406.

Niimura H, Yokoyama T, Kimura S, Matsumoto Y, Kuga S (2010) AFM observation of ultrathin microfibrils in fruit tissues. Cellulose 17:13-18.

Parameswaran BN, Liese W (1976) On the fine structure of bamboo fibers. Wood Sci Technol 10:231-246.

Pesacreta TC, Carlson LC, Triplett BA (1997) Atomic force microscopy of cotton fiber cell wall surfaces in air and water: Quantitative and qualitative aspects. Planta 202:435-442.

Silva JLG, Al-Qureshi HA (1999) Mechanics of wetting systems of natural fibers with polymeric resin. J Mater Process Technol 92(93):124-128.

Thimm JC, Burritt DJ, Ducker WA, Melton LD (2000) Celery parenchyma cell walls examined by atomic force microscopy: Effect of dehydration on cellulose microfibrils. Planta 212:25-32.

Thimm JC, Burritt DJ, Ducker WA, Melton LD (2009) Pectins influence microfibril aggregation in celery walls: An atomic force microscopy study. J Struct Biol 168(2):337-344.

Wang G, Shi QS, Wang JW, Cao SP, Cheng HT (2011) Tensile of properties of four tupes of individual cellulosic fibers. Wood Fiber Sci 43(4):353-364.

Weissler A (1984) Ultrasonics in chemistry. J Chem Educ 25(1):28-30.

Yu Y, Jiang ZH, Wang G, Qin DC, Cheng Q (2008a) Visualization of cellulose microfibrils of Moso bamboo fibers with atomic force microscopy. J Beijing For Univ 30(1):124-127.

Yu H, Liu RG, Shen DW, Wu ZH, Huang Y (2008b) Arrangement of cellulose microfibrils in the wheat straw cell wall. Carbohyd Polym 72:122-127.

Zhang L, Chen F, Yang H, Ye X, Sun X, Liu D (2012) Effect of temperature and cultivar on nanostructural changes of water-soluble pectin and chelate-soluble pectin in peaches. Carbohyd Polym 87:816-821.

Zhou BL (1996) Some progress in the biomimetic study of composite materials. Mater Chem Phys 45(2):114-119.

Zimmermann T, Thommen V, Reimann P, Hug HJ (2006) Ultrastructural appearance of embedded and polished wood cell walls as revealed by Atomic Force Microscopy. J Struct Biol 156:363-369.

Zou LH, Jin H, Lu WY, Li X (2009) Nanoscale structural and mechanical characterization of the cell wall of bamboo fibers. Mater Sci Eng C 29:1375-1379.